

# Investigating Broad Absorption Line Quasars with SDSS and UKIDSS

N. Maddox<sup>1\*</sup>, P.C. Hewett<sup>2</sup>  
\*nmaddox@aip.de

<sup>1</sup> Astrophysikalisches Institut Potsdam, Germany  
<sup>2</sup> Institute of Astronomy, Cambridge, UK



## 1 Introduction

The fraction of quasars exhibiting broad absorption lines (BALs) in their spectra blueward of high ionisation lines, primarily CIV, is poorly constrained, with several authors arriving at seemingly discrepant results. A complete census of the BAL quasar (BALQSO) population will help constrain both the absorber geometry and covering fraction, and determine the contribution of the BALQSO phase to AGN feedback and thus the co-evolution of supermassive black hole and host galaxy growth.

There are indications that BALQSOs have somewhat redder continua than nonBALQSOs [8, among others]. If the reddening is due to dust associated with the quasars, then the number of BALQSOs present in optically selected samples is an underestimate of the total population. Observations at longer wavelengths less affected by dust extinction, such as the NIR, alleviate this issue. This study aims to exploit the overlap between the SDSS and the newly available large area, deep NIR data provided by UKIDSS to investigate the NIR properties of BALQSOs, the optical–NIR colours of BALQSOs with respect to the nonBALQSO population, and constrain the shape of the extinction curve causing the reddening.

## 2 Data

The optical photometry and spectra are taken from the SDSS DR5 quasar catalogue [10]. These 77429 quasars are then matched to data contained within the UKIDSS Large Area Survey (LAS) DR3+ [6], limited to  $K \leq 17.0$  (Vega). Only quasars within the redshift range  $1.70 \leq z \leq 4.38$  are retained to ensure spectral coverage of the CIV 1549Å emission line and the blueward continuum, resulting in a final sample of 2051 objects. This redshift range coincides with that used in the SDSS DR3 BAL study of Trump et al. 2006 [11].

As one aim of this study is to determine whether BALQSOs are redder than the nonBALQSO population, the reddest objects must be included. Figure 1 illustrates the  $i$ - $K$  values accessible at a series of  $K$ -band magnitude limits for the SDSS Main Survey area (top) and the Stripe 82 area only (bottom). Comparing the top and bottom panels shows that the deeper Stripe 82 data, which isn't subjected to the  $i \leq 18.7$  (Vega) magnitude limit of the SDSS quasar selection algorithm, reaches larger  $i$ - $K$  values for a given  $K$ -band magnitude. Therefore, for statistical purposes, the sample is divided into three subsamples. Stripe 82 data is used for  $K \leq 17$  and  $K \leq 16$  subsamples, and the SDSS Main Survey area is used for  $K \leq 15$  statistics. The  $K \leq 17$  subsample from the Stripe 82 data is found to suffer from incompleteness due to the limited  $i$ - $K$  range, but included for illustration.

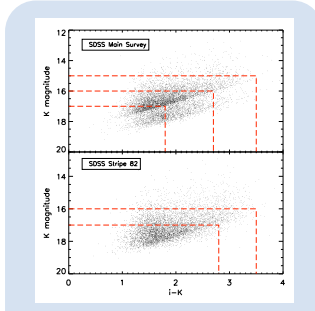


**Figure 1:** Colour-magnitude diagrams for matched SDSS-UKIDSS quasars, showing only data from the SDSS Main Survey area (top) and from the SDSS Stripe 82 area (bottom). The density ridge seen in the top panel is from the  $i \leq 18.7$  (Vega) magnitude restriction in the quasar selection algorithm. The deeper  $i$ -band limit within the Stripe 82 data allows uniform access to objects with larger  $i$ - $K$  colours for a given  $K$ -band magnitude.

## Balnicity Index

In order to compute the balnicity index (BI), a 'continuum fit' is required. A high SNR composite quasar spectrum was constructed from a large number of nonBALQSOs. Each quasar spectrum is divided by the redshifted composite, and a power-law fit ( $f_{\lambda} \propto \lambda^{\alpha}$ ) is used to characterise the difference in slope between the quasar and composite spectra. The overall shape of the composite spectrum is adjusted using the power-law fit. Then, an iterative procedure further modifies the shape of the composite on smaller scales using the systematic differences between the composite and the quasar spectra that fall below the adjusted composite by more than a specified threshold (i.e. broad absorption lines) are excluded from the fitting process. The BI is then computed for each continuum-normalised spectrum, using the formula described in Appendix A of Weymann et al. 1991 [12]. Any object with  $BI > 2$  is classified as a BALQSO.

## 3 Optical-NIR Colour

Figure 2 shows the  $i$ - $K$  colours as a function of redshift for the full sample of 2051  $K \leq 17$  quasars, with BALQSOs shown as open circles. A  $K$ - $S$  test on the  $K \leq 16$  sample indicates that the  $i$ - $K$  colours of BALQSOs are redder than the colours of the nonBALQSO population with high significance, with the  $i$ - $K$  distribution for the BALQSOs having a more extended red tail. Overplotted are quasar tracks derived from a model quasar as described in Maddox et al. 2008 [7]. The black line shows the  $i$ - $K$  colour for an unreddened quasar, with the thick blue, green and red lines indicating the colours for the model quasar subjected to increasing amounts of SMC-like dust reddening. If the reddening of the BALQSOs is due to dust, the position of an object on the  $i$ - $K$  vs redshift plane provides an estimate of the amount of extinction it is suffering.

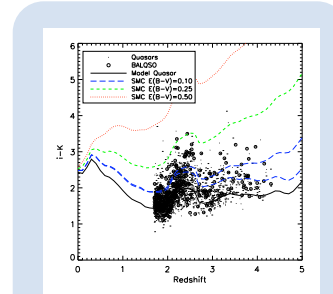


**Figure 2:** The  $i$ - $K$  vs redshift colours of the full sample of 2051  $1.7 \leq z \leq 4.38$ ,  $K \leq 17$  quasars, with BALQSOs shown as open circles. The solid black line indicates the  $i$ - $K$  colour for a typical unobscured model quasar, the blue long dashed line indicates the same model quasar reddened by SMC-like dust with  $E(B-V)=0.10$ , the green short dashed line is the model quasar reddened with  $E(B-V)=0.25$  and the red dotted line is the model quasar reddened with  $E(B-V)=0.50$ . The thin blue dashed line indicates the colour of the model quasar reddened by dust as described in Gaskell & Benker 2007 [2], which has a shallower slope at short wavelengths.

## 4 BALQSO Fraction

Estimates of the fraction of BALQSOs with respect to the entire quasar population range from  $\sim 10\%$  [11] to corrected fractions of  $> 20\%$  [3, 5]. Recent work by Dai et al. 2008 [1], using the SDSS DR3 BALQSO list compiled by Trump et al. 2006 [11] in conjunction with NIR data from 2MASS shows that the BALQSO fraction increases as the quasar sample is selected at longer wavelengths. Although the Dai et al. result uses the expanded definition of BALQSO as introduced by Trump et al. 2006, the nature of the result remains relevant to this work.

	SDSS Main Survey Area			SDSS Stripe 82			KX
	N <sub>TOTAL</sub>	N <sub>BALQSO</sub>	F <sub>BALQSO</sub>	N <sub>TOTAL</sub>	N <sub>BALQSO</sub>	F <sub>BALQSO</sub>	F <sub>BALQSO</sub>
$K \leq 17$	1426	205	14%	625	106	17%	15%
$K \leq 16$	291	54	19%	93	25	27%	25%
$K \leq 15$	28	5	18%	14	2	14%	---

The computed uncorrected BALQSO fractions for the various subsamples are compiled in Table 1. The  $K \leq 17$  BALQSO fractions are underestimates, due to their restricted range in  $i$ - $K$  colour. The  $K \leq 15$  fraction from the SDSS Main area is almost certainly affected by small number statistics. The  $K \leq 16$  fraction in the Stripe 82 area reaches large  $i$ - $K$  values and relatively faint  $K$ -band magnitude, while including a statistically significant number of objects, and thus provides the best estimate of the BALQSO fraction. The value of  $\sim 27\%$  is significantly larger than the  $\sim 10\%$  found using the SDSS DR3 sample, and is in good agreement with results from Maddox et al. 2008 [7], who find a BALQSO fraction of  $\sim 25\%$  from a sample of quasars selected based on their  $K$ -band excess. As these samples are flux-limited in the  $K$ -band, the corrections due to dust obscuration, if that is indeed the cause of their red colours, is small, and changes the BALQSO fractions only by a few percent, in contrast with the large corrections that are needed at optical wavelengths.

## 5 Composite Spectra

Assuming an object's position on the  $i$ - $K$  vs redshift plot (Figure 2) is entirely due to dust reddening,  $E(B-V)$  values for each quasar can be computed, and the population divided according to the amount of reddening suffered. Quasars with  $E(B-V) < 0.05$  are designated as unreddened, objects with  $0.05 < E(B-V) < 0.1$  mildly reddened, and those with  $E(B-V) > 0.1$  moderately reddened. Composite spectra are created for each of the three categories. Both BALQSOs and nonBALQSOs are included in the composites. The results do not change if only BALQSOs are included, only the signal-to-noise ratio of the composites is lower due to fewer contributing spectra.

Dividing the reddened composite spectra by the unreddened composite effectively produces extinction curves. The top panel of Figure 3 shows the mildly reddened composite ratio spectrum, overlaid with a dust reddening curve assuming dust of the form from Gaskell & Benker 2007 [2] with an  $E(B-V)$  value representative of the objects used to create the composite. As seen, the Gaskell & Benker curve is not red enough at short ( $\lambda < 2200\text{\AA}$ ) wavelengths. The discrepancy increases with the moderately reddened composite. The bottom panel shows the moderately reddened composite ratio spectrum overlaid with an SMC-type dust extinction curve. The SMC curve is too red at short wavelengths.

The extinction curve required to fit the moderately reddened composite therefore has SMC-type behaviour at  $\lambda > 2000\text{\AA}$ , but a less steep rise at shorter wavelengths, possibly indicating a reduced fraction of very small dust grains. There is also no evidence for a 2175Å feature as found in Galactic or LMC curves.

## 6 Conclusions

Combining data from SDSS and UKIDSS it is apparent that BALQSOs have redder optical–NIR colours than the nonBALQSO population. The fraction of the quasar population exhibiting the BAL phenomenon in samples selected in the  $K$ -band is found to be as high as 27%, much larger than the 10% found in optically selected samples. This result is in agreement with the 25% BALQSO fraction found in the large area,  $K$ -band excess selected quasar sample of Maddox et al. 2008 [7].

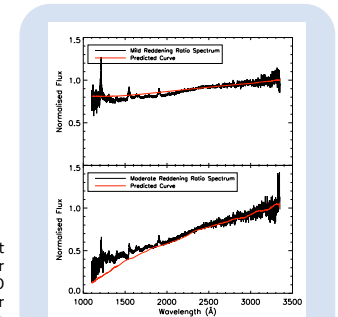


**Figure 3:** (Top) Composite spectrum created from mildly reddened quasars, divided by composite spectrum of unreddened objects, with an extinction curve assuming dust of the form of Gaskell & Benker 2007 [2]. (Bottom) Composite spectrum created from moderately reddened quasars, divided by composite spectrum of unreddened objects, with an extinction curve assuming SMC-type dust.

Dividing composite spectra created from quasars with red  $i$ - $K$  colours by an unreddened composite indicates that the reddening is not consistent with either SMC-type dust or dust as postulated by Gaskell & Benker 2007 [2]. The extinction curve appears similar to that of the SMC at  $\lambda > 2000\text{\AA}$ , but is much less steep at shorter wavelengths. This is in contrast with several studies based on SDSS quasars [4,9] that find the reddest quasars to have spectral shapes consistent with SMC-type dust. However, these studies focus on lower redshift quasars, and are therefore not as sensitive to the departure from SMC dust behaviour seen at  $\lambda < 2000\text{\AA}$  in Figure 3.

## References

- [1] Dai, X., et al., ApJ, 672, 108, 2008
- [2] Gaskell, C.M., Benker, A.J., astro-ph 0711.1013
- [3] Hewett, P.C., Foltz, C.B., AJ, 125, 1784, 2003
- [4] Hopkins, P.F., et al., AJ, 128, 1112, 2004
- [5] Knigge, C., et al., MNRAS, 386, 1426, 2008
- [6] Lawrence, A., et al., MNRAS, 379, 1599, 2007
- [7] Maddox, N., et al., MNRAS, 386, 1605, 2008
- [8] Reichard, T.A., et al., AJ, 126, 2594, 2003
- [9] Richards, G.T., et al., AJ, 126, 1131, 2003
- [10] Schneider, D.P., et al., AJ, 134, 102, 2007
- [11] Trump, J.R., et al., ApJS, 165, 1, 2006
- [12] Weymann, R.J., et al., ApJ, 373, 23, 199